Wedge wetting by van der Waals fluids

M. Napiórkowski,* W. Koch, and S. Dietrich
Fachbereich Physik, Bergische Universität Wuppertal, Postfach 100127, D-5600 Wuppertal 1, Germany
(Received 13 August 1991)

Using a microscopic density-functional theory for inhomogeneous van der Waals fluids, we derive the equation for the shape of the interface between a liquidlike adsorbed film and the vapor phase in the bulk exposed to a long-range potential of a wedge-shaped substrate. This is a nonlinear and nonlocal integral equation associated with the line tension of the system. Within certain approximations it reduces to that equation which follows from the common phenomenological approach for bent interfaces between fluid phases. The asymptotic lateral behavior of the interfacial profile far away from the center of the wedge displays the presence of van der Waals tails; they are calculated analytically for the cases of complete and critical wetting. The full solutions of the integral equation are obtained numerically. They allow us to predict a scaling behavior of the excess coverage as a function of the thickness of the wetting layer far away from the center of the wedge.

PACS number(s): 68.45.Gd, 68.10.−m, 68.55.Jk, 68.35.Rh

I. INTRODUCTION

The phenomenon of wetting of a flat, homogeneous, and chemically inert substrate by a liquid coexisting with its vapor is rather well understood [1–3]. In the absence of corrugations of the substrate the main geometrical feature of the adsorbed liquidlike layer is given by its thickness l. It depends on the thermodynamic state of the fluid and—parametrically—on the fluid-fluid and fluid-substrate interaction potentials. The density profile orthogonal to the flat substrate remains close to a constant value given by the bulk liquid density up to $z \simeq l$ where it smoothly crosses over towards the vapor density in the bulk. This latter transition region resembles the *intrinsic* structure of the free liquid-vapor interface whose thickness is given by the bulk correlation length ξ, whereas the bulk values are attained by van der Waals tails. One may define the mean position of this emerging interface and thus the thickness of the liquidlike layer as the distance from the substrate to the inflection point of the profile (see Figs. 1 and 3 in Ref. [4]). Upon changing the thermodynamic state of the fluid in a specifically chosen way one may induce an unlimited growth of the thickness l; this signals a wetting phase transition of the substrate-vapor interface. If this growth is induced by approaching the liquid-vapor coexistence curve from the vapor side it is called complete wetting. If the growth takes place upon changing the state of the fluid along the liquid-vapor coexistence line towards a specific point with the so-called wetting temperature T_w it is called either critical wetting corresponding to a continuous growth of l or first-order wetting corresponding to a discontinuous jump of l to a macroscopic value. These different kinds of wetting behavior can be described transparently by introducing the concept of the effective interface potential defined as the substrate-vapor surface tension under the constraint that the liquidlike wetting layer has a prescribed thickness l [4–6].

The preparation of atomically flat and homogeneous substrates requires enormous experimental efforts. Ordinarily, one is always confronted with a certain amount of geometrical and chemical disorder. As a consequence the interface bound to the substrate has to adjust itself locally to this disorder so that one encounters nontrivial shapes of interfaces, e.g., in systems in which the bulk of the fluid is exposed to a random environment [7,8], in the case of wetting of a fractal [9–12], rough [13], inhomogeneous [14,15], or stepped [16–19] substrate, in the case of adsorption in pores [20–22] or when discussing the rupture of thin liquid films [23]. Wedge wetting [24–26] serves as a paradigm for such nontrivial interfacial profiles. Also, wetting of artificially patterned surfaces, which have broad practical applications, belongs to the above category of problems. Corner-wetting studies in lattice models with short-range forces [27] are a first step in understanding the emerging structures microscopically as a function of bulk and surface fields. However, as stressed by those authors, these results sensitively depend on the lattice structure of the model and are not applicable to continuous-fluid systems, which therefore require a different approach (see below).

Until now wetting phenomena in nonstandard geometries and the structure of the emerging interfacial shapes were analyzed mainly within phenomenological models. In these studies one refrains from determining the full fluid-density profile. Instead, one is interested in the mean position of the interface and how it adjusts itself to the shape of the substrate. Within this phenomenological approach the equation for the mean position of the interface is obtained by minimizing a free-energy functional constructed in such a way as to include, among other contributions, the cost in free energy related to the distortion of a flat interface in the absence of external fields. This cost is described phenomenologically [28] by

$$\Delta \mathcal{F} = \sigma_{lg} \int_A d^2\rho (\{1+[\nabla F(\boldsymbol{\rho})]^2\}^{1/2}-1) , \quad (1)$$

where the single-valued function $F(\rho)$ denotes the mean position of the interface as function of the lateral coordinates ρ within a flat reference area A. In Eq. (1) this cost in free energy $\Delta\mathcal{F}$ is taken to be the product of the surface tension σ_{lg} between the coexisting liquid and vapor phases and the increase in area of the interface due to distortion. Under certain assumptions the effective interface model in Eq. (1) can be derived from bulk models [29–33] and it amounts to neglecting curvature contributions. After minimization of the phenomenological expression for the free energy—which contains in addition to $\Delta\mathcal{F}$ also terms describing the interaction of the interface with the substrate—one obtains a local differential equation for the actual profile $\bar{F}$.

Recently, $\Delta\mathcal{F}$ has been calculated starting from a microscopic theory of liquids [34]. It turns out that Eq. (1) is in fact replaced by a *nonlocal* functional of $F(\rho)$ which effectively contains arbitrarily high-order derivatives of $F(\rho)$ [34]; Eq. (1) can be retrieved in a certain approximate sense. Naturally, the question arises how important the difference is between Eq. (1) and the actual nonlocal expression for $\Delta\mathcal{F}$. In order to probe this difference quantitatively we apply the approach of Ref. [34] to wedge wetting, expecting that the resulting shapes $\bar{F}$ of the emerging interface within the wedge are sensitive to the actual nonlocal character of $\Delta\mathcal{F}$.

Therefore we study the problem of wetting in a nonstandard geometry by deriving systematically an effective interface model from a microscopic theory of fluids. For the latter we take a particular form of a grand-canonical density functional [35] and apply it to a one-component fluid whose particles interact via long-range van der Waals forces exposed to a long-range substrate potential of the same character. The specific geometry of the substrate, which we take as a testing ground for our aforementioned general goal, is formed by two interpenetrating, semi-infinite flat walls meeting at an angle of 90° (see Fig. 1). This wedge is assumed to have a uniform number density ρ_w occupying the volume

$$\Lambda_w=\{\mathbf{r}=(\rho,z)=(x,y,z)\in\mathbb{R}^3 | y\le |x|-\sqrt{2}d_w\}\ .$$

[Due to the repulsive part of the substrate potential the density profiles vanish for distances which are closer to the top layer of the substrate than d_w; see Fig. 4.1(a) in Ref. [1] and cf. Eq. (24a).] It is translationally invariant in the z direction; accordingly, the mean interface position is also translationally invariant in this direction. Within our systematic microscopic approach we obtain a nonlinear and nonlocal equation for the mean shape of the interface $\bar{F}(x)$. We shall show under which conditions it reduces to the phenomenological equation commonly used in the literature and how the predictions stemming from these two approaches compare with each other. The asymptotic behavior of the profile for $x\to\pm\infty$ can be inferred analytically from the nonlocal equation and the results turn out to differ from those derived from the phenomenological approach. We shall present also numerical solutions of this nonlocal equation and discuss the scaling properties of the amount of liquid adsorbed in the wedge as function of the asymptotic layer thickness l (see Fig. 1).

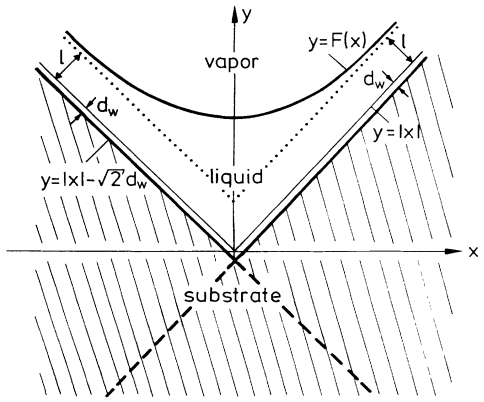

FIG. 1. Structure of the wedge and an interface configuration given by $y=F(x)$. The dotted line corresponds to $y=|x|+\sqrt{2}l$ which is the required asymptote of $F(x)$; l denotes the thickness of the liquidlike layer adsorbed on the same but flat substrate. Within the dashed line the two semi-infinite flat walls forming the substrate overlap; in the text this region is denoted by Λ_w^o. Due to the repulsive part of the substrate potential there is an excluded volume of thickness d_w near the surface. (In order to obtain the thickness of the wetting film according to the notation used in Refs. [1] and [4–6] one has to add d_w.)

II. EQUATION FOR THE INTERFACIAL PROFILE

Our analysis is based on the mean-field density-functional theory [35]. In this approach the number density $\rho(\mathbf{r})$ of the fluid filling the wedge is determined by minimizing the grand-canonical free-energy functional,

$$\Omega[\{\rho(\mathbf{r})\};T,\mu]=\int d^3r\, f_h(\rho(\mathbf{r}),T) + \tfrac{1}{2}\int d^3r\int d^3r'\,\bar{w}(|\mathbf{r}-\mathbf{r}'|)\rho(\mathbf{r})\rho(\mathbf{r}') + \int d^3r[\rho_w V(\mathbf{r})-\mu]\rho(\mathbf{r})\ . \quad (2)$$

The regions of integration are given by $\mathbb{R}^3\setminus\Lambda_w$ (see Appendix A). The spherically symmetric pair potential $w(|\mathbf{r}|)$ that describes the interaction between the fluid particles is separated into a long-range attractive part and a short-range repulsive part. $\bar{w}(|\mathbf{r}|)$ describes the long-range attractive part decaying like r^{-6}; at short distances we adopt the Weeks-Chandler-Andersen (WCA) procedure [36]. Accordingly, the repulsive part of the interaction at small distances is taken into account by introducing a reference system of hard spheres; $f_h(\rho,T)$ is the corresponding bulk Helmholtz free-energy density of a homogeneous system of hard spheres with number density ρ; μ denotes the chemical potential. In Eq. (2) the reference free energy is evaluated in the local-density approximation [37]. The interaction of the fluid particle with the wedge is described by the substrate potential $\rho_w V(\mathbf{r})=\rho_w\bar{V}(x,y)$, which at large distances from the wedge also contains a long-range attractive part.

In order to obtain the mean position $y=\bar{F}(x)$ of the interface we minimize $\Omega[\{\rho(\mathbf{r})\};T,\mu]$ within the subspace of density configurations $\rho(\mathbf{r})=\hat{\rho}(x,y)$ which are translationally invariant in the z direction and are given by the following sharp-kink expression:

$$\hat{\rho}(x,y)=\Theta(y-|x|)\{\rho_l\Theta(F(x)-y)+\rho_g\Theta(y-F(x))\} . \tag{3}$$

ρ_l and ρ_g denote the number densities of the bulk liquid and vapor phases, respectively; Θ is the Heaviside function. We want to emphasize that although the emerging liquid-vapor interface is curved, there is no pressure difference between the liquidlike film and the vapor in the bulk because the total volume of the liquidlike film is unbounded. Therefore all physical quantities are independent from the choice of a dividing surface between the two phases which may be identified by Eq. (3) (see Ref. [38]).

After inserting $\hat{\rho}(x,y)$ into Eq. (2), Ω reduces to a functional of $F(x)$ and of the fluid-fluid and fluid-substrate interaction potentials. Ω is also a function of μ, T, and the flat substrate wetting layer thickness l which enters via the requirement $F(x\to\pm\infty)=|x|+\sqrt{2}l$ for the asymptotic behavior of the profile. For a fluid system of finite size $L_x\times L_y\times L_z$ (see Appendix A) in the thermodynamic limit $L_z\to\infty$ with $L=L_x=L_y$ the free-energy functional decomposes into a bulk (Ω_b), a surface (Ω_s), and a line (Ω_l) contribution:

$$\begin{aligned}\lim_{L_z\to\infty}\frac{1}{L_z}\Omega[\{\hat{\rho}(x,y)\};T,\mu] &= L^2\Omega_b(\rho_g;T,\mu)+2L\Omega_s(l;\rho_l,\rho_g,T,\mu)\\ &\quad+\Omega_l[\{F(x)\};l,\rho_l,\rho_g,T,\mu]+O(L^{-1}) .\end{aligned} \tag{4}$$

(Note that in this limit the area of the substrate is given by $2L\times L_z$.) The detailed expressions for Ω_b, Ω_s, and Ω_l are given in Appendix A. An important property of Eq. (4) is that the different types of contributions depend on different characteristics of the density configuration $\hat{\rho}(x,y)$. The bulk contribution depends only on the bulk density ρ_g. The actual values $\bar{\rho}_l$ and $\bar{\rho}_g$ minimize $\Omega_b(\rho;T,\mu)$. They are functions of the thermodynamic state of fluid, i.e., $\bar{\rho}_l=\bar{\rho}_l(T,\mu)$ and $\bar{\rho}_g=\bar{\rho}_g(T,\mu)$. In the case of critical wetting they are evaluated along the coexistence line $\mu=\mu_0(T)$. In the case of complete wetting, which corresponds to approaching the coexistence line from the vapor side, we take $\bar{\rho}_l(T,\mu_0(T))$ and $\bar{\rho}_g(T,\mu)$, i.e., we evaluate the bulk liquid density at the coexistence line and the bulk vapor density off the coexistence line. The surface contribution $\Omega_s(l;\rho_l,\rho_g,T,\mu)$ is identical to the surface free energy for the corresponding semi-infinite flat substrate [see Eqs. (4.9)–(4.11) in Ref. [1]] and depends on the asymptotic layer thickness l and—parametrically—on ρ_l and ρ_g. The actual value $\bar{l}$ minimizes Ω_s with respect to l with the known values $\bar{\rho}_l$ and $\bar{\rho}_g$. Thus the wetting temperature T_w and other wetting properties of the system such as $\bar{l}$ are fixed by Ω_s. Finally, only the contribution Ω_l depends on the interfacial profile $F(x)$ and—parametrically—on ρ_l, ρ_g, and l. The condition $\delta\Omega_l/\delta F(x)=0$ with $\rho_l=\bar{\rho}_l$, $\rho_g=\bar{\rho}_g$, and $l=\bar{l}$ renders the following equation for the actual interfacial profile $\bar{F}(x)$:

$$\begin{aligned}\Delta\Omega=&\Delta\rho[\rho_l\bar{t}(x,\bar{F}(x))-\rho_w\bar{V}(x,\bar{F}(x))]\\ &-(\Delta\rho)^2\int_{-\infty}^{+\infty}dx'\int_0^{\bar{F}(x')-\bar{F}(x)}dy'\,\hat{w}(x'-x,y') ,\end{aligned} \tag{5}$$

where

$$\hat{w}(x,y)=\int_{-\infty}^{\infty}dz\,\bar{w}((x^2+y^2+z^2)^{1/2}) , \tag{6}$$

$\Delta\rho=\bar{\rho}_l-\bar{\rho}_g$, and $\Delta\Omega=\Omega_b(\bar{\rho}_l,T,\mu)-\Omega_b(\bar{\rho}_g,T,\mu)=\Delta\rho\Delta\mu+O((\Delta\mu)^2)$ with $\Delta\mu=\mu_0(T)-\mu\geq 0$. In the case of critical wetting $\Delta\Omega=0$ so that the remaining temperature dependence resides in $\rho_l(T,\mu_0(T))$ and $\Delta\rho(T,\mu_0(T))$. The function $\bar{t}(x,y)$ is proportional to the interaction energy between a fluid particle located at a point (x,y,z) and the wedge $\{(x,y,z)\in\mathbb{R}^3|y\leq|x|\}$ formed by the *fluid* [for a precise definition see Eq. (A12)]. It is thus completely analogous to the interaction energy $\bar{V}(x,y)$ between a fluid particle and the wedge formed by the actual substrate. These two functions enter Eq. (5) only via the difference

$$U(x,y)=\rho_l\bar{t}(x,y)-\rho_w\bar{V}(x,y) . \tag{7a}$$

In general, one has

$$\bar{V}(x,y)=V\left[\frac{y+x}{\sqrt{2}}\right]+V\left[\frac{y-x}{\sqrt{2}}\right]-\Delta V\left[\frac{y+x}{\sqrt{2}},\frac{y-x}{\sqrt{2}}\right] \tag{7b}$$

due to the following physical interpretation: $V(z)$ is the potential energy of a fluid particle located a distance z apart from a semi-infinite flat substrate. $\Delta V((y+x)/\sqrt{2},(y-x)/\sqrt{2})$ describes the interaction of a fluid particle located at a point (x,y,z) with that part of the wedge which is formed by the overlap region

$$\Lambda_w^o=\{(x,y,z)\in\mathbb{R}^3|y\leq-|x|-\sqrt{2}d_w\}$$

of the two semi-infinite flat walls (see Fig. 1). An analogous formula holds for $\bar{t}(x,y)$:

$$\bar{t}(x,y)=t\left[\frac{y+x}{\sqrt{2}}\right]+t\left[\frac{y-x}{\sqrt{2}}\right]-\Delta t\left[\frac{y+x}{\sqrt{2}},\frac{y-x}{\sqrt{2}}\right] . \tag{7c}$$

$t(z)$ and $\Delta t(z,z')$ [see Eqs. (A13) and (A14)] are the analogs of $V(z)$ and $\Delta V(z,z')$, respectively. In order to avoid a clumsy notation in the following we drop the bar over ρ_l, ρ_g, l, and $F(x)$ denoting the actual equilibrium values.

The thermodynamic singularities of wetting transitions of van der Waals fluids at flat substrates are known to be captured correctly by mean-field theories [39]. The study of wedge wetting requires the minimization of the line contribution to the free-energy functional in contrast to minimizing a surface contribution in the case of a flat geometry. Thus, effectively, wedge wetting corresponds

to a lower-dimensional problem than wetting of a flat substrate, and so the criterion for the applicability of mean-field theory should be reanalyzed. This analysis is deferred to future studies.

Equation (5) is a nonlinear and nonlocal integral equation for the interfacial profile $F(x)$. The nonlocality is due to the second term on the right-hand side (rhs) of this equation. It can be proved that for smooth interfacial profiles describing locally small deviations of the actual interface from a flat one [Eq. (5)] may be cast rigorously into the following local form:

$$\Delta\Omega-\Delta\rho U(x,F(x))=\sigma_{lg}\frac{d^2F(x)}{dx^2}\left[1+\left[\frac{dF(x)}{dx}\right]^2\right]^{3/2} +\text{higher-order terms} . \quad (8)$$

As a by-product the derivation of Eq. (8) yields a microscopic expression for the liquid-vapor surface tension σ_{lg} which is given in Eq. (A4). Here, the higher-order terms contain at least the square of $d^2F(x)/dx^2$ or third-order derivatives of F. For this rather tedious proof one uses the spherical symmetry of the potential $\tilde{w}(r)$ and expands the difference $F(x')-F(x)$ into powers of $x'-x$. Then the integrations are carried out and a subsequent partial resummation of the resulting series in powers of the derivatives of F renders the rhs of Eq. (8) [34]. Equations analogous to Eq. (8) are encountered in phenomenological approaches, where the cost in free energy for deforming a flat interface is taken to be the surface tension times the increase in area. [Note that the first term on the rhs of Eq. (8) equals the functional derivative of $\Delta\mathcal{F}$ as given in Eq. (1).] Our microscopic approach goes not only beyond this local approximation but it yields also a microscopically defined expression for the left-hand side (lhs) of Eq. (8). This microscopic interpretation of the lhs of the above phenomenological equation has so far been missing in the literature.

III. van der WAALS TAILS OF THE INTERFACIAL PROFILE

For realistic long-range particle-particle and particle-substrate interaction potentials the integral equation, Eq. (5), can be solved only numerically. These results are presented in Sec. IV. In this section we discuss the behavior of the interfacial profiles at large distances from the center of the wedge. In order to obtain analytic formulas describing this asymptotic behavior it is useful to rewrite the interfacial profile in the following form:

$$F(x)=\sqrt{2}l+|x|+f(x) . \quad (9)$$

The function $f(x)=f(-x)$ characterizes the excess thickness of the wetting film compared with its thickness on a flat substrate. Therefore far away from the center of the wedge one has $f(x=\pm\infty)=0$. If the thermodynamic conditions (at fixed interaction potentials) are chosen in such a way that the thickness l of the wetting film on the flat substrate is large compared to the diameter d of the particles, the asymptotic behavior of the function $f(x)$ is given in the limits

$$l/d\to\infty,\quad x/d\to\infty,\quad l/d\ll(x/d)^{3/5} \quad (10a)$$

by the power law

$$f(x\to\infty)=f_0/x^3 \quad (10b)$$

to which we refer to as the van der Waals tails of the shape of the interface. [The third condition in Eq. (10a) follows from the requirement $f_0x^{-3}\ll d$ and the results for f_0 given in Eq. (15).] Their presence is induced by the power-law decay of the interaction potential [40]. The asymptotic behavior of $f(x)$, Eq. (10b), follows from Eq. (5) by using Eqs. (9), (7a), and (7b). Then, on the rhs of Eq. (5) the following terms stemming from $U(x,F(x))$, Eq. (7a), are present:

$$I_1=\Delta\rho\left[\rho_l t\left[l+\frac{|x|+x+f(x)}{\sqrt{2}}\right]-\rho_w V\left[l+\frac{|x|+x+f(x)}{\sqrt{2}}\right]\right],$$

$$I_2=\Delta\rho\left[\rho_l t\left[l+\frac{|x|-x+f(x)}{\sqrt{2}}\right]-\rho_w V\left[l+\frac{|x|-x+f(x)}{\sqrt{2}}\right]\right],$$

and

$$I_3=\Delta\rho\left[\rho_w\Delta V\left[1+\frac{|x|+x+f(x)}{\sqrt{2}},l+\frac{|x|-x+f(x)}{\sqrt{2}}\right]-\rho_l\Delta t\left[l+\frac{|x|+xf(x)}{\sqrt{2}},l+\frac{|x|-x+f(x)}{\sqrt{2}}\right]\right].$$

After using the equation $\partial\Omega_s/\partial l=0$ for the flat geometry, which determines the equilibrium value $\bar{l}$ of l, one obtains—in the limits given by Eq. (10a)—the following results: $I_1\sim x^{-3}$, $I_2=\Delta\Omega+\text{const}\times f(x)$, and $I_3\sim x^{-3}$ [see Eqs. (22c) and (24b)]. In the same limits the double integral on the rhs of Eq. (5) is proportional to x^{-3}. These results induce the behavior of $f(x)$ given in Eq. (10b).

As already mentioned in the Introduction fluids interacting via long-range forces exhibit another type of van der Waals tails *within* the intrinsic structure of interfaces (see Refs. [1] and [4], and references therein). These

characterize the approach of the fluid number density towards its bulk values. If z denotes the distance from the mean position of a flat interface this decay is given asymptotically by $\rho(z\to\infty)-\rho(\infty)\sim z^{-3}$, where $\rho(z)$ denotes the value of the number density at a distance z from the interface. Such van der Waals tails are—in addition—also present in the wedge problem. However, because we are only interested in the mean position of the interface we employ the sharp-kink approximation [see Eq. (3)], which discards these intrinsic van der Waals tails.

The amplitude f_0 is determined by inserting the asymptotic behavior in Eq. (10) into Eqs. (9), (7), and (5) and by analyzing Eq. (5) in the aforementioned limits. Before quoting the results for f_0 we recall some relevant facts about wetting phenomena on flat substrates.

The limit $l\to\infty$ corresponds either to the case of complete wetting, i.e., $T_w<T<T_c$, $\mu_0-\mu=\Delta\mu\searrow 0$, or to the case of critical wetting, i.e., $\Delta\mu=0^+$, $T\nearrow T_w$. For complete wetting the asymptotic growth law is given by

$$l(\Delta\mu\searrow 0, T>T_w)=\left[\frac{\rho_w u_3-\rho_l t_3}{\Delta\mu}\right]^{1/3}, \tag{11}$$

where $\rho_w u_3>\rho_l(T>T_w)t_3$. The coefficients u_3 and t_3 are determined by the asymptotic behavior of the functions $t(x)$ and $V(x)$:

$$t(x)=-\frac{t_3}{x^3}-\frac{t_4}{x^4}-\cdots,\quad t_3>0\,, \tag{12a}$$

$$V(x)=-\frac{u_3}{x^3}-\frac{u_4}{x^4}-\cdots,\quad u_3>0\,. \tag{12b}$$

In the case of critical wetting the wetting temperature T_w is given by the implicit equation

$$\rho_w u_3=\rho_l(T=T_w)t_3\,, \tag{12c}$$

with the asymptotic growth law (note that the definition of l used in Fig. 1 differs from that in Refs. [1] and [4–6])

$$l(T\nearrow T_w,\Delta\mu=0^+)=\frac{\rho_w u_4-\rho_l t_4}{\rho_l t_3-\rho_w u_3}\sim\left[\frac{T_w-T}{T_w}\right]^{-1}. \tag{13}$$

Critical wetting occurs if the conditions $\rho_w u_3<\rho_l(T<T_w)t_3$, $\rho_w u_4>\rho_l(T=T_w)t_4$, and Eq. (12c) are fulfilled [4].

Following the procedure mentioned above one obtains in the case of complete wetting

$$f_0^{\rm comp}=\frac{1}{12}l^4\frac{\rho_g t_3-\rho_w u_3}{\rho_l t_3-\rho_w u_3}\geq\frac{1}{12}l^4\,, \tag{14}$$

where ρ_g and ρ_l are evaluated at coexistence and l is given by Eq. (11). For critical wetting one has

$$f_o^{\rm crit}=\frac{1}{4}l^5\frac{\rho_g t_3-\rho_w u_3}{\rho_l t_4-\rho_w u_4}\,, \tag{15}$$

where ρ_g and ρ_l are evaluated at $T=T_w$ and l is given by Eq. (13). According to Eq. (14) the amplitude $f_0^{\rm comp}$ is positive so that the profile $F(x)$ approaches its asymptote $|x|+\sqrt{2}l$ from above. Also, in the case of critical wetting the amplitude $f_0^{\rm crit}$ is positive (see Appendix B). Due to the requirement $f_0 x^{-3}\ll d$, one sees that in the case of complete wetting the condition $l/d\ll(x/d)^{3/5}$ [see Eq. (10a)] can be actually relaxed to $l/d\ll(x/d)^{3/4}$. One should note that the van der Waals tails in Eq. (10a) will be present for all values of l, but for small l with different values of f_0 than those given in Eqs. (14) and (15).

Within the local approximation [see Eq. (8)] the asymptotic behavior of the profile is again given by Eq. (10), but the expressions for the amplitudes f_0 differ from those of nonlocal theory [see Eqs. (14) and (15)]. In the case of complete wetting one obtains

$$\hat{f}_0^{\rm comp}=\tfrac{1}{12}l^4\,, \tag{16}$$

while in the case of critical wetting one has

$$\hat{f}_o^{\rm crit}=-\tfrac{1}{4}l^4\,. \tag{17}$$

The difference between these two results, Eqs. (14) and (15) and Eqs. (16) and (17), highlights the weakness of the local approximation in Eq. (8) which predicts, *inter alia*, the wrong sign of the van der Waals tail amplitude in the case of critical wetting and always underestimates the strength of the van der Waals tails in the case of complete wetting.

IV. NUMERICAL DETERMINATION OF THE INTERFACIAL PROFILES

As already pointed out, the full solution of Eq. (5) can be obtained only numerically. First, we want to note that in the special case $l=\infty$, which corresponds to the free liquid-vapor interface, Eq. (5) has the simple solution

$$f(x)=c-|x|\,, \tag{18}$$

where c is an arbitrary constant. Thus the arbitrariness of c reflects the fact that in the absence of external fields the mean position of the free interface separating two coexisting phases is not determined [28].

In order to obtain the numerical solution of Eq. (5) for $l<\infty$ we have to specify the fluid-fluid, $\bar{w}(r)$, and the fluid-substrate, $\bar{V}(x,y)$, interaction potentials as well as an equation of state for the hard-sphere reference fluid, $p_h(\rho,T)$, which enters the van der Waals equation of state

$$p(\rho,T)=p_h(\rho,T)-\tfrac{1}{2}w_0\rho^2\,, \tag{19a}$$

where the constant w_0 is the integrated strength of the attractive part of the fluid-fluid interaction potential:

$$w_0=\int_{-\infty}^{\infty}dx\int_{-\infty}^{\infty}dy\;\hat{w}(x,y)\,. \tag{19b}$$

For the hard-spheres equation of state we use the Carnahan-Starling equation [41],

$$p_h(\rho,T)=k_B T\rho\frac{1+\eta+\eta^2-\eta^3}{(1-\eta)^3}\,, \tag{20a}$$

$$\eta=\tfrac{1}{6}\pi\rho d^3\,, \tag{20b}$$

where d is the hard-sphere diameter. As our model for

the fluid-fluid interaction potential $\hat{w}(r)$ we adopt, in the spirit of the WCA procedure [36], the following expression:

$$\hat{w}(r)=w_0\frac{4d^3}{\pi^2}(d^2+r^2)^{-3} . \tag{21}$$

[Note that in the strict WCA sense one would have $\tilde{w}(r\le d)=\tilde{w}(d)$. We adopt Eq. (21) because it closely resembles the strict WCA potential and enables us in addition to perform one of the two integrations in Eq. (5) analytically.] The hard-sphere diameter d sets the microscopic length scale. In the following lengths are measured in units of d and densities in units of d^{-3}. The choice of Eq. (21) leads to

$$\hat{w}(x,y)=w_0\frac{3}{2\pi d^2}(1+\bar{x}^2+\bar{y}^2)^{-5/2} , \tag{22a}$$

$$t(x)=\frac{w_0}{\pi}\left[\frac{\pi}{2}-\arctan(\bar{x})-\frac{\bar{x}}{1+\bar{x}^2}\right] , \tag{22b}$$

and

$$\Delta t(x,y)=\frac{w_0}{2\pi}\left[\frac{\pi}{2}-\arctan(\bar{x})-\frac{\bar{x}}{1+\bar{x}^2}-\arctan(\bar{y})-\frac{\bar{y}}{1+\bar{y}^2}+\arctan\left[\frac{\bar{x}\,\bar{y}}{(1+\bar{x}^2+\bar{y}^2)^{1/2}}\right]+\frac{\bar{x}\,\bar{y}}{1+\bar{x}^2+\bar{y}^2+\bar{x}^2\bar{y}^2}\left[(1+\bar{x}^2+\bar{y}^2)^{1/2}+\frac{1}{(1+\bar{x}^2+\bar{y}^2)^{1/2}}\right]\right] , \tag{22c}$$

where $\bar{x}=x/d$ and $\bar{y}=y/d$. The parameter t_3 defined in Eq. (12a) can be expressed in terms of w_0 and d as

$$t_3=-\frac{2}{3}\frac{w_0 d^3}{\pi} . \tag{22d}$$

For the interaction potential $\tilde{w}_{fs}(r)$ between a fluid particle and a substrate particle we adopt the following model [1,42]:

$$\tilde{w}_{fs}(r)=4\epsilon_w\left[\frac{\sigma_w}{r}\right]^{12}-\frac{6u_3}{\pi}(d^2+r^2)^{-3}-\frac{10}{\pi}\left[u_4+\frac{3u_3}{2}(\sigma_w+d)\right](d^2+r^2)^{-7/2} . \tag{23}$$

The first term on the rhs of Eq. (23) describes the repulsion at short distances and σ_w denotes the diameter of the substrate particles. The two remaining terms describe the attraction at large distances. The inclusion of terms proportional to u_4 in Eq. (23) is necessary in order to be able to discuss wedge wetting in the case of critical wetting [see Eq. (15)]. Equation (23) leads to the following form of the potential $V(x)$ describing the interaction of a fluid particle with a homogeneous and flat semi-infinite substrate

$$V(x)=\frac{4\pi\epsilon_w d^3}{45}\left[\frac{\sigma_w}{d}\right]^{12}\hat{x}^{-9}+\frac{u_3}{t_3}t(x+(\sigma_w+d)/2)-\frac{4}{3d^4}\left[u_4+\frac{3u_3}{2}(\sigma_w+d)\right]\left[2-\frac{\hat{x}(3+2\hat{x}^2)}{(1+\hat{x}^2)^{3/2}}\right] , \tag{24a}$$

where $\hat{x}=\bar{x}+(\sigma_w+d)/2d$. $V(x)$ diverges at $x=-(\sigma_w+d)/2$ and has a zero close to $x=0$. Thus the density profiles vanish for $x\lesssim 0$. This corresponds to the density configuration indicated in Fig. 1 with $d_w=\frac{1}{2}(\sigma_w+d)$. Via the equation $\partial\Omega_s/\partial l=0$ the potentials $t(x)$ and $V(x)$ determine the equilibrium value of l in the flat geometry [see Eq. (A2)]. In our numerical analysis the parameters ϵ_w, σ_w, u_3, t_3, and u_4 in Eqs. (21) and (23) for the potentials $\tilde{w}(r)$ and $\tilde{w}_{fs}(r)$ are arranged in such a way that continuous wetting indeed occurs and that asymptotically the equilibrium value of l is given by Eqs. (11) and (13) where in turn only the asymptotic characteristics of these potentials enter. (Note that due to our choice of $\tilde{w}(r)$ in Eq. (21), $t_4=0$ [see Eq. (12a)].) According to our previous findings [see Eqs. (7a)–(7c), (9), and (14) and Appendix B] for such large values of l the shape of the interface profile satisfies the inequality $F(x)>l$. Therefore in Eq. (5) the expressions for $\bar{V}(x,y)$ and $\bar{t}(x,y)$ are evaluated only at large values of their arguments. Thus in our numerical analysis we can employ the asymptotic form of the potentials $V(x)$ and $\Delta V(x,y)$; for $\Delta V(x,y)$ one has ($\hat{y}=\bar{y}+d_w/d$)

$$\Delta V(x,y)=\frac{u_3}{t_3}\Delta t(x+d_w,y+d_w)-\frac{u_4+3d_w u_3}{\pi d^4}\left\{\frac{1}{\hat{x}^4}\left[\frac{\pi}{2}-\arctan\left[\frac{\hat{y}}{\hat{x}}\right]\right]+\frac{1}{\hat{y}^4}\arctan\left[\frac{\hat{y}}{\hat{x}}\right]-\frac{8}{3}\frac{1}{\hat{x}\hat{y}(\hat{x}^2+\hat{y}^2)}-\frac{(\hat{x}^2-\hat{y}^2)^2}{\hat{x}^3\hat{y}^3(\hat{x}^2+\hat{y}^2)}\right\},\quad \hat{x},\hat{y}\gg 1 . \tag{24b}$$

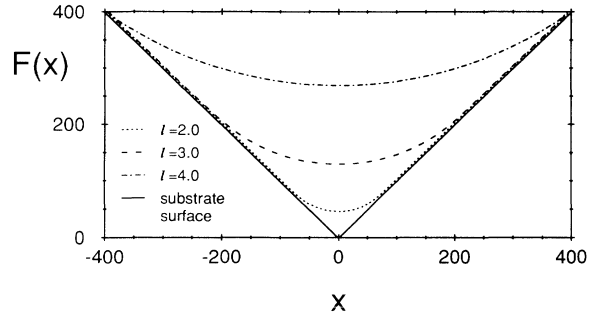

FIG. 2. Three interfacial profiles $F(x)$ calculated numerically for different values of the parameter l in the case of *complete wetting*; x, $F(x)$, and l are measured in units of the hard-sphere diameter d of the fluid particles. The profiles were determined for the following values of our parameters: $u_3/|w_0|d^3=0.146$, $u_4=0$, $\sigma_w=d$, $\epsilon_w d^3/|w_0|=0.635$, and $T/T_c=0.773$. For these parameters one has $d_w=d$, $T_w/T_c=0.724$, $T/T_w=1.068$, $u_3/t_3=0.688$, $k_B T_c/|w_0|d^{-3}=0.098$, $\rho_l d^3=0.647$, and $\rho_g d^3=0.040$ at coexistence. Due to the choice of $\bar{w}$ in Eq. (21) one has $t_4=0$. The three curves correspond to $\Delta\mu/k_B T_c=0.0118$, 0.0035, and 0.0015, respectively. On the scale of this figure the excluded volume is not visible.

After determining the liquid-vapor coexistence curve $\mu_0(T)$, the liquid and vapor densities $\rho_l(T,\mu)$ and $\rho_g(T,\mu)$, respectively, the wetting temperature T_w, and—within the sharp-kink approximation used in this paper—the thickness $l(T,\mu)$ of the wetting layer in the flat geometry one has all the necessary input data in order to be able to solve Eq. (5) numerically for the interfacial profile $f(x)$. The numerical solutions, which we obtained using a standard procedure for solving an integral equation, are presented in Figs. 2 and 3. Figure 2 corresponds to complete wetting with $l/d=2$, 3, and 4. Figure 3 corresponds to critical wetting with $l/d=2$, 2.5, and 3. In both cases we observe a substantial increase of the profile $F(x)$ with increasing l. This behavior is reflected by the strong increase of the van der Waals tails as function of l [see Eqs. (14) and (16)]. This sets an upper limit for the values of l which are numerically accessible. Having determined numerically the full interfacial profiles for different values of l, we calculated the excess coverage (as compared to the flat geometry) given by the integral

$$\Gamma=\int_{-\infty}^{\infty} f(x)dx \ , \tag{25}$$

which depends on l [see Fig. 4(a)]. Our extensive numerical analysis shows that in the limit of large l—as far as it is numerically accessible—it obeys a scaling behavior

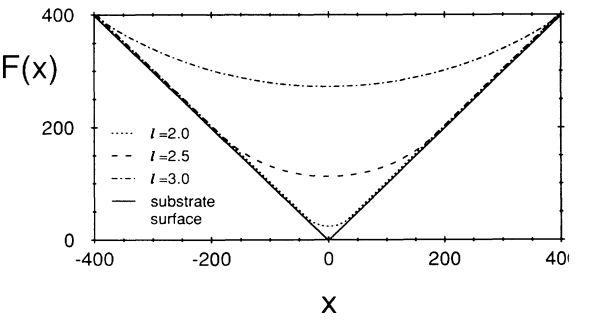

FIG. 3. Three interfacial profiles $F(x)$ calculated numerically for different values of the parameter l in the case of *critical wetting*; x, $F(x)$, and l are measured in units of the hard-sphere diameter d. The profiles were determined for the following values of our parameters: $u_3/|w_0|d^3=0.113$, $u_4/|w_0|d^4=0.090$, $\sigma_w=d$, and $\epsilon_w d^3/|w_0|=0.591$. For these parameters on has $d_w=d$, $T_w/T_c=0.879$, $u_3/t_3=0.530$, $k_B T_c/|w_0|d^{-3}=0.098$, $\rho_l(T_w)d^3=0.533$, and $\rho_g(T_w)d^3=0.084$ at coexistence; $t_4=0$. The three curves correspond to $(T_w-T)/T_w=0.192$, 0.181, and 0.146, respectively. On the scale of this figure the excluded volume is not visible.

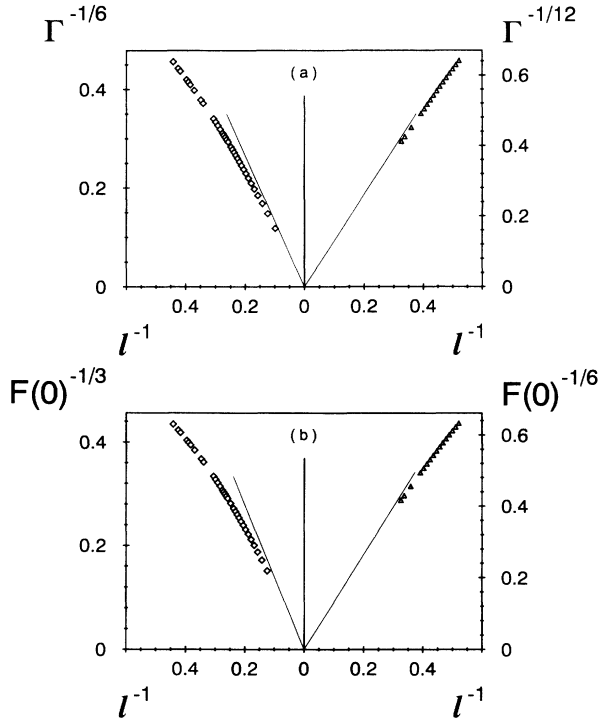

FIG. 4. The excess coverage Γ and the thickness $F(0)$ of the wetting film in the center of the wedge as a function of l for large l. (a) $\Gamma^{-1/\kappa}$ plotted as a function of l^{-1} for complete wetting ($\kappa=6$, $\Diamond$) and for critical wetting ($\kappa=12$, $\triangle$). Γ and l are measured in units of d^2 and d, respectively. (b) $F(0)^{-2/\kappa}$ plotted as a function of l^{-1} for complete wetting ($\kappa=6$, $\Diamond$) and for critical wetting ($\kappa=12$, $\triangle$). $F(0)$ and l are measured in units of d. These data are obtained for the following set of parameters: $u_3/|w_0|d^3=0.146$, $u_4=0$, $u_3/t_3=0.688$, $t_4=0$, $\sigma_w=d$, $\epsilon_w d^3/|w_0|=0.635$, $T_w/T_c=0.724$, $T/T_w=1.068$, and $k_B T_c/|w_0|d^{-3}=0.098$ for complete wetting, and $u_3/|w_0|d^3=0.127$, $u_4/|w_0|d^3=0.020$, $u_3/t_3=0.596$, $t_4=0$, $\sigma_w=d$, $\epsilon_w d^3/|w_0|=0.574$, $T_w/T_c=0.724$, and $k_B T_c/|w_0|d^{-3}=0.098$ for critical wetting. As the asymptotes suggest the coverage Γ and the thickness $F(0)$ follow the scaling law $\Gamma(l\to\infty)=\gamma l^{\kappa}$ and $F(0;l\to\infty)=F_0 l^{\kappa/2}$ with $\gamma=0.335d^{-4}$, $F_0=0.551d^{-2}$ for complete wetting, and $\gamma=0.043d^{-10}$, $F_0=0.207d^{-5}$ for critical wetting, respectively.

$$\Gamma(l\to\infty)=\gamma l^{\kappa} . \tag{26}$$

The numerical data are consistent with $\kappa=6$ for complete wetting and $\kappa=12$ for critical wetting. The result $\kappa=6$ for complete wetting was suggested recently [26] on the basis of the phenomenological equation for the interfacial profile which was solved by approximating the actual interfacial profile by a semicircle joining tangentially the asymptotes. Although in this approximation the presence of van der Waals tails in the shape of the interface is disregarded the asymptotic behavior of the excess coverage as a function of l is reproduced correctly. This approximate analysis also suggests that in the case of complete wetting the value of κ is determined by the exponent characterizing the asymptotic decay of the interparticle potential $\tilde{w}(r)\sim r^{-\lambda}$ according to $\kappa=2(\lambda-3)$.

We also checked the scaling behavior of $F(0)$, i.e., the thickness of the liquidlike film at the center of the wedge as a function of l [see Fig. 4(b)]. Both for complete and critical wetting we find

$$F(0;l\to\infty)=F_0 l^{\kappa/2} . \tag{27}$$

This result suggests that in the asymptotic regime $l\to\infty$ the excess coverage $\Gamma(l)$ and the thickness $F(0,l)$ of the wetting layer at the wedge center are related according to $\Gamma(l)\sim[F(0,l)]^2$. Thus for large l the morphology of the wetting film in a wedge is characterized by a single length scale as for a flat substrate.

V. CONCLUSIONS

Under suitable thermodynamic conditions liquidlike films can be formed at wall-vapor interfaces. Both the thickness and the shape of such thin films have to adjust themselves locally to lateral inhomogeneities of the substrates which can occur on very different length scales ranging from atomic sizes up to micrometers. Up to now such readjustments of films have been studied theoretically by simple phenomenological models. Since meanwhile such structures can be probed experimentally on an atomic scale, e.g., by x-ray scattering [43] and atomic force microscopy [44,45], it has become necessary to refine the corresponding theoretical treatment by basing it on statistical mechanics.

For the particular example of a wedge as a simple lateral inhomogeneity we have analyzed systematically a suitable microscopic theory of inhomogeneous fluids [Eq. (2)] in order to determine the equilibrium shape of the liquidlike film as a function of the thermodynamic variables and as a functional of the basic interaction potentials. This amounts to studying the line contribution to the free-energy functional of the fluid interacting with the wedge (Appendix A). The resulting complicated integral equation [Eq. (5)] for this shape of the substrate can be studied analytically far away from the center of the wedge where van der Waals tails appear [Eqs. (10), (14), and (15)] which are induced by the long-range character of both the substrate potential and the adsorbate-adsorbate interaction potential in van der Waals fluids. It turns out that even in this asymptotic regime, where the interface varies only slightly, the predictions of the phenomenological models, which can be recovered as an approximation to the aforementioned integral equation [Eq. (8)], are wrong both quantitatively and qualitatively [Eqs. (16) and (17)]. Close to wetting transitions the wedge is rather rapidly filled by the liquid, so that the extra coverage due to the wedge increases $\sim l^{\kappa}$, where l is the thickness of the wetting layer on a corresponding flat substrate. The exponent κ depends on the character of the wetting transition. For van der Waals fluids with nonretarded forces $\kappa=6$ for complete wetting and $\kappa=12$ for critical wetting. In both cases the thickness of the film at the center of the wedge increases $\sim l^{\kappa/2}$ [Eq. (27)].

On the basis of these results several further improvements of the theoretical analysis can be envisaged. One can choose more-sophisticated density functionals than the one used in Eq. (2). In addition, the intrinsic structure of the emerging liquid-vapor interface should be taken into account in order to overcome the sharp-kink approximation in Eq. (3). Furthermore, it would be interesting to focus on fluctuations, both capillary waves at low temperatures and critical fluctuations close to the critical point of the fluid [46]. Nonartificial wedges have a finite depth so that the strong increase of the coverage will come to a natural end which raises interesting questions concerning crossover phenomena due to an extra vertical length scale. The change of the opening angle of the wedge necessarily leads to additional crossover phenomena.

Finally, we would like to mention that there have been already experimental attempts to analyze fluids confined to a wedgelike geometry [47,48]. Thus we are slightly optimistic that a detailed interferrometric study either by laser light or by x rays will allow one to test our specific theoretical predictions of the growth of thin films in a wedge.

ACKNOWLEDGMENTS

Helpful discussions with D. Beaglehole, V. Privman, and M. Schick are gratefully acknowledged.

APPENDIX A

In order to separate the grand-canonical density functional Ω into its bulk, surface, and line contribution we consider a fluid system which is infinite along the z direction, finite in the x-y plane, and interacting with the infinite wedgelike substrate. We assume that the fluid is contained within the following region:

$$\{(x,y,z)\in\mathbb{R}^3 | -L/\sqrt{2}<x<L/\sqrt{2};|x|-\sqrt{2}d_w<y<\sqrt{2}L-|x|\}$$

(see Fig. 5). Thus the line $y=\sqrt{2}L-|x|$ defines the position of the artificial fluid-vacuum interface. Using the expression in Eq. (3) for the density profile, one arrives after tedious calculations at the following expressions for the bulk (Ω_b), surface (Ω_s), and line [$\Omega_l \equiv \Omega_{\text{line}}(l)$] contribution (here and in the following the expression l for the thickness of the wetting film should not be confounded with the abbreviation l for the line contribution and liquid, respectively):

$$\Omega_b(\rho_g;T,\mu)=f_h(\rho_g,T)+\tfrac{1}{2}w_0\rho_g^2-\mu\rho_g \tag{A1}$$

and

$$\Omega_s(l;\rho_l,\rho_g,T,\mu)=\Omega_s^g(l)+\sigma_{gv} \tag{A2}$$

where

$$\Omega_s^g(l)=l\Delta\Omega+\Delta\rho\int_l^\infty dx\,[\rho_l t(x)-\rho_w V(x)]+\sigma_{wl}+\sigma_{lg}\ . \tag{A3}$$

The wall-gas surface tension σ_{wg} is the minimum value of $\Omega_s^g(l)$: $\sigma_{wg}=\min_l\Omega_s^g(l)=\Omega_s^g(l=\bar{l})$. The line contribution can be divided naturally into three distinct terms:

$$\Omega_{\text{line}}[\{F(x)\};l,\rho_l,\rho_g,T,\mu]=\tilde{\Omega}_{\text{line}}[\{F(x)\}]+\omega_{\text{line}}+\Delta\omega_{\text{line}}\ . \tag{A4}$$

$\Delta\omega_{\text{line}}$ is introduced artificially by the cutoff used in order to obtain a finite size of the system [see Eqs. (A15)–(A20)]:

$$\Delta\omega_{\text{line}}=-2l(\sigma_{gv}-\sigma_{lv})+2\tau_{lwwv}+2\tau_{lvvg}+\tau_{vgvv}\ . \tag{A5}$$

The term ω_{line} is independent from the density configuration and contains a constant and an l-dependent contribution:

$$\omega_{\text{line}}=\tau_{\text{liquid}}+l^2\Delta\Omega-2l(\Omega_s^g(l)-\sigma_{wl})-\Delta\rho\int_l^\infty dx\int_l^\infty dy\,[\rho_l\Delta t(x,y)-\rho_w\Delta V(x,y)]-2\Delta\rho\rho_l\int_l^\infty dx\int_0^\infty dy\,\Delta t(x,y) \tag{A6}$$

with [see Eqs. (A15)–(A20)]

$$\tau_{\text{liquid}}=\tau_{wwwl}+\tau_{lllg}\ . \tag{A7}$$

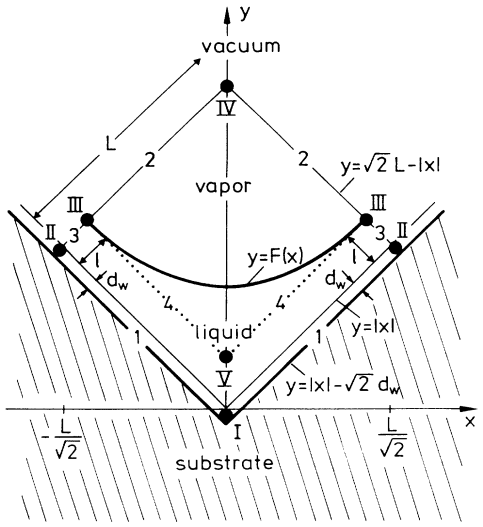

FIG. 5. The same as Fig. 1 but for a finite-size ($L\times L$) fluid system in the x-y plane. The finite size of the system allows us to indicate the surface and line tensions defined in Appendix A [see Eqs. (A8)–(A10) and (A15)–(A18)]. The line tensions are denoted by roman numbers and the surface tensions are denoted by arabic numbers: I, τ_{wwwl}; II, τ_{lwwv}; III, τ_{lvvg}; IV, τ_{vgvv}; 1, σ_{wl}; 2, σ_{gv}; 3, σ_{lv}. In the case $f(x)=0$ the surface tension $\sigma_{lg}(\equiv 4)$ and the line tension $\tau_{lllg}(\equiv V)$ can also be indicated in this figure. Similarly, as in Fig. 1 the distances l, d_w, and L are indicated by arrows.

The constant contribution τ_{liquid} can be identified as the line tension [49,50] for the wedge filled by the liquid phase only. Note that for large l the l-dependent contribution grows asymptotically proportional to l^2 in distinction to the linear l dependence of the surface term in Eq. (A3); this is in accordance with a simple dimensional analysis.

$\tilde{\Omega}_{\text{line}}$ contains all the dependence of the line contribution on the shape of the liquid-vapor interface. Therefore Eq. (5) follows from minimizing $\tilde{\Omega}_{\text{line}}[\{F(x)\}]$ with respect to $F(x)$. The explicit expression for $\tilde{\Omega}_{\text{line}}$ is given by

$$\tilde{\Omega}_{\text{line}}[\{F(x)\}]=\Delta\Omega\Gamma-\Delta\rho\int_{-\infty}^{\infty}dx\int_{|x|+\sqrt{2}l}^{F(x)}dy\,[\rho_l\bar{t}(x,y)-\rho_w\bar{V}(x,y)]+\tfrac{1}{2}(\Delta\rho)^2\left[\int_{-\infty}^{\infty}dx\int_{|x|+\sqrt{2}l}^{F(x)}dy\,\bar{t}(x,y-\sqrt{2}l)+\int_{-\infty}^{\infty}dx\int_{F(x)}^{|x|+\sqrt{2}l}dy\int_{-\infty}^{\infty}dx'\int_{F(x')}^{\infty}dy'\,\hat{w}(x-x',y-y')\right], \tag{A8}$$

where Γ is the excess coverage defined in Eq. (25). The line tension τ of the system is given by $\tau=\omega_{\text{line}}+\tilde{\Omega}_{\text{line}}$ evaluated at the equilibrium values of l and $F(x)$.

Within the sharp-kink approximation the expression for the liquid-vapor surface tension σ_{lg} has the following form [4]:

$$\sigma_{lg}=-\tfrac{1}{2}(\Delta\rho)^2\int_0^\infty dx\,t(x) \tag{A9}$$

and

$$\sigma_{lv}=-\tfrac{1}{2}\rho_l^2\int_0^\infty dx\,t(x) \tag{A10}$$

is the liquid-vacuum surface tension. An expression analogous to Eq. (A10) holds for the vapor-vacuum surface tension σ_{gv} with ρ_l replaced by ρ_g. The wall-liquid surface tension σ_{wl} is given by

$$\sigma_{wl}=-\tfrac{1}{2}\rho_l^2\int_0^\infty dx\, t(x)+\rho_l\rho_w\int_0^\infty dx\, V(x)\ . \quad \text{(A11)}$$

(Note that $V(x\to 0)$ is finite [see Eq. (24a)]; σ_{wl} depends via $V(x)$ on d_w and thus on our treatment of the excluded volume effect indicated in Fig. 1.) In Eqs. (A6)–(A11) we have introduced the following abbreviations:

$$\bar{t}(x,y)=\int_{-\infty}^{\infty}dx'\int_{-\infty}^{|x'|}dy'\,\hat{w}(x-x',y-y')\ , \quad \text{(A12)}$$

$$t(x)=\int_x^\infty dx'\int_{-\infty}^{\infty}dy'\,\hat{w}(x',y')\ , \quad \text{(A13)}$$

and

$$\Delta t(x,y)=\int_x^\infty dx'\int_y^\infty dy'\,\hat{w}(x',y')\ . \quad \text{(A14)}$$

The quantities $\tau_{\alpha\beta\gamma\delta}$ occurring in Eqs. (A5) and (A7) are defined as

$$\tau_{wwwl}=\tfrac{1}{2}\rho_l^2\Delta\tau-\rho_l\rho_w\Delta v\ , \quad \text{(A15)}$$

$$\tau_{lwwv}=\tfrac{1}{2}\rho_l^2\Delta\tau\ , \quad \text{(A16)}$$

$$\tau_{lllg}=\tau_{lvvg}=\tfrac{1}{2}(\Delta\rho)^2\Delta\tau\ , \quad \text{(A17)}$$

$$\tau_{vgvv}=\tfrac{1}{2}\rho_g^2\Delta\tau \quad \text{(A18)}$$

with

$$\Delta\tau=\int_0^\infty dx\int_0^\infty dy\,\Delta t(x,y) \quad \text{(A19)}$$

and

$$\Delta v=\int_0^\infty dx\int_0^\infty dy\,\Delta V(x,y)\ . \quad \text{(A20)}$$

The meaning of the subscripts $\alpha,\beta,\gamma,\delta$ in Eqs. (A15)–(A20) is self-explanatory: All four phases denoted by $\alpha,\beta,\gamma,\delta$—each of them contained in a quarter of space—meet along a line common to all of them. $\tau_{\alpha\beta\gamma\delta}$ are the line tensions associated with these configurations. The subscript w stands for wall (i.e., substrate), l for liquid, g for vapor, and v for vacuum. The line tensions τ_{wwwl}, τ_{lwwv}, τ_{lllg}, τ_{lvvg}, τ_{vgvv}, and the surface tensions σ_{wl}, σ_{lg}, σ_{gv}, and σ_{lv} are indicated schematically in Fig. 5.

APPENDIX B

Critical wetting requires the fulfillment of three conditions: $\rho_l(T=T_w)t_3<\rho_w u_4$, $\rho_l(T<T_w)t_3>\rho_w u_3$, and $\rho_l(T=T_w)t_3<\rho_w u_3$. Thus the condition $f_0^{\rm crit}<0$ [see Eq. (15)] is equivalent to the condition $\rho_l t_3-\rho_w u_3>\Delta\rho t_3$ where both sides of the inequality are positive. For $T\nearrow T_w<T_c$ the lhs of this inequality vanishes, whereas the rhs of the inequality attains the positive value $\Delta\rho(T=T_w)t_3$, which leads to a contradiction. Consequently, close to T_w, $f_0^{\rm crit}$ is positive. However, one cannot rule out the possibility that f_0 may be negative at lower temperatures.

*Permanent address: Institute for Theoretical Physics, Warsaw University, Hoża 69, 00-681 Warszawa, Poland.

[1] S. Dietrich, in *Phase Transitions and Critical Phenomena,* edited by C. Domb and J. L. Lebowitz (Academic, London, 1988), Vol. 12, p. 1.
[2] D. E. Sullivan and M. M. Telo da Gama, in *Fluid Interfacial Phenomena,* edited by C. A. Croxton (Wiley, New York, 1986), p. 45.
[3] M. Schick, in *Liquids at Interfaces,* Les Houches Summer School Lectures, Session XLVIII, edited by J. Chavrolin, J. F. Joanny, and J. Zinn-Justin (Elsevier, Amsterdam, 1990), p. 415.
[4] S. Dietrich and M. Napiórkowski, Phys. Rev. A **43**, 1861 (1991).
[5] S. Dietrich, in *Phase Transitions in Surface Films 2,* edited by H. Taub (Plenum, New York, 1991), p. 391.
[6] M. Napiórkowski and S. Dietrich, Europhys. Lett. **9**, 361 (1989).
[7] M. E. Fisher, J. Chem. Soc., Faraday Trans. 2 **82**, 1569 (1968).
[8] G. Forgacs, R. Lipowsky, and Th. M. Nieuwenhuizen, in *Phase Transitions and Critical Phenomena,* edited by C. Domb and J. L. Lebowitz (Academic, London, in press), Vol. 14.
[9] E. Cheng, M. W. Cole, and A. L. Stella, Europhys. Lett. **8**, 527 (1989).
[10] P. Pfeifer, Y. J. Wu, M. W. Cole, and J. Krim, Phys. Rev. Lett. **62**, 1997 (1989).
[11] M. Kardar and J. O. Indekeu, Europhys. Lett. **12**, 161 (1990).
[12] G. Guigliarelli and A. L. Stella, Phys. Scr. **T35**, 34 (1991).
[13] D. Andelman, J. F. Joanny, and M. O. Robbins, Europhys. Lett. **7**, 731 (1988).
[14] M. Robbins, D. Andelman, and J. F. Joanny, Phys. Rev. A **43**, 4344 (1991).
[15] M. W. Cole and E. Vittoratos, J. Low Temp. Phys. **22**, 223 (1976).
[16] E. V. Albano, K. Binder, D. W. Heermann, and W. Paul, Surf. Sci. **223**, 151 (1989).
[17] E. V. Albano, K. Binder, D. W. Heermann, and W. Paul, Z. Phys. B **47**, 445 (1989).
[18] A. C. Levi and E. Tosatti, Surf. Sci. **178**, 425 (1986).
[19] G. Bilalbegović, V. Privman, and N. M. Švrakić, J. Phys. A **22**, L833 (1989).
[20] M. W. Cole and M. Schmeits, Surf. Sci. **75**, 529 (1978).
[21] A. J. Liu, D. J. Durian, E. Herbolzheimer, and S. A. Safran, Phys. Rev. Lett. **65**, 1897 (1990).
[22] R. Evans, U. Marini Bettolo Marconi, and P. Tarazona, J. Chem. Soc. Faraday Trans. 2 **82**, 1763 (1986).
[23] A. Sharma and E. Ruckenstein, J. Colloid Interface Sci. **133**, 358 (1990).
[24] B. V. Derjaguin and N. V. Churaev, J. Colloid Interface Sci. **54**, 157 (1976).
[25] Y. Pomeau, J. Colloid Interface Sci. **113**, 5 (1985).
[26] E. Cheng and M. W. Cole, Phys. Rev. B **41**, 9650 (1990).
[27] P. M. Duxbury and A. C. Orrick, Phys. Rev. B **39**, 2944

(1989).
[28] D. Jasnow, Rep. Prog. Phys. **47**, 1059 (1984).
[29] H. W. Diehl, D. M. Kroll, and H. Wagner, Z. Phys. B **36**, 329 (1980).
[30] S. C. Liu and M. J. Lowe, J. Phys. A **16**, 347 (1983).
[31] M. D. A. Fisher and M. Wortis, Phys. Rev. B **29**, 6252 (1984).
[32] R. K. P. Zia, Nucl. Phys. B **251** [FS13], 676 (1985).
[33] J. B. Keller and G. J. Merchant, J. Stat. Phys. **63**, 1039 (1991).
[34] S. Dietrich and M. Napiórkowski, Physica A **177**, 437 (1991).
[35] R. Evans, Adv. Phys. **28**, 143 (1979).
[36] J. Barker and D. Henderson, Rev. Mod. Phys. **48**, 587 (1976).
[37] There are various nonlocal approximations; see, e.g., M. Baus, J. Phys.: Condens. Matter **2**, 2111 (1990); D. M. Kroll and B. B. Laird, Phys. Rev. A **42**, 4806 (1990), and references therein.
[38] B. Widom, in *Proceedings of The Gibbs Symposium, Yale University, 1989* (American Mathematical Society, Providence, RI, 1990), p. 73.
[39] S. Dietrich, M. P. Nightingale, and M. Schick, Phys. Rev. B **32**, 3182 (1985).
[40] Here, similar arguments hold as given by P. G. de Gennes [J. Phys. (Paris) Lett. **42**, L377 (1981)] for van der Waals tails *within* the intrinsic structure of interfaces.
[41] J. P. Hansen and I. R. McDonald, *Theory of Simple Liquids* (Academic, London, 1986).
[42] Ph. Lambin, A. A. Lucas, I. Derycke, J.-P. Vigneron, and E. G. Derouane, J. Chem. Phys. **90**, 3814 (1989).
[43] I. M. Tidswell, T. A. Rabedeau, P. S. Pershan, and S. D. Kosowsky, Phys. Rev. Lett. **66**, 2108 (1991).
[44] C. M. Mate, M. R. Lorenz, and V. J. Novotny, J. Chem. Phys. **90**, 7550 (1989).
[45] M. L. Forcada, M. M. Jakas, and A. Gras-Marti, J. Chem. Phys. **95**, 706 (1991).
[46] J. L. Cardy, J. Phys. A **16**, 3617 (1983); Nucl. Phys. B **240**, [FS12], 514 (1984); J. L. Cardy and S. Redner, J. Phys. A **17**, L933 (1984); V. K. Saxena, Phys. Rev. B **35**, 3612 (1987); B. Davis and I. Peschel, J. Phys. A **24**, 1293 (1991); H. W. Diehl, in *Phase Transitions and Critical Phenomena,* edited by C. Domb and J. L. Lebowitz (Academic, London, 1986), Vol. 10, p. 65, Subsec. IV A 3.
[47] M. R. Moldover and R. W. Gammon, J. Chem. Phys. **80**, 528 (1984).
[48] D. Beysens, in *Liquids at Interfaces,* Les Houches Summer School Lectures, Session XLVIII, edited by J. Chavrolin, J. F. Joanny, and J. Zinn-Justin (Elsevier, Amsterdam, 1990). p. 499.
[49] J. S. Rowlinson and B. Widom, *Molecular Theory of Capillarity* (Oxford University, Oxford, 1982), Chap. 8.
[50] B. Widom and H. Widom, Physica A **173**, 72 (1991).